Received: 01-11-2013
Accepted: 21-12-2013

ISSN: 2321-4902
Volume 1 Issue 4

Online Available at www.chemijournal.com

International Journal of Chemical Studies

Removal and Kinetics of Oxalic Acid Adsorption from Aqueous Waste over Alkali Activated Power Plant Fly Ash

M. Dakshene[1]*, A. Rani[2], P.D. Sharma[3]

1. Department of Chemistry, Govt. College, Kota, India
2. Department of Pure & Applied Chemistry, University of Kota, Kota, India
3. Department of Chemistry, University of Rajasthan, Jaipur, India

*[Email: monika.dakshene@gmail.com, Tel. No: +919928146739]

Oxalic acid is a chemical that is commonly used in the production of lubricant component, plasticizers, pharmaceutical, and rubber industries. Effluent emitted from these industries contain this chemical is a major cause of pollution in water system and is hazardous to the living beings. This chemical is reported to cause pain, tearing in eyes, skin irritation etc. Fly ash from coal burning power plant was activated chemically, used as a low cost adsorbent for the removal of oxalic acid, which is a major cause of pollution in water system. The activated fly ash was characterized for mineralogical, physiochemical and morphological properties by XRD, FT-IR and SEM. Results showed that activated fly ash due to increased amorphous property possesses more activity over surface to act as a suitable adsorbent for the removal of acidic waste from individual effluents. The adsorption kinetics is well represented by first order kinetic model.

Keyword: Chemical activation, fly ash, oxalic acid, adsorption.

1. Introduction

Oxalic acid, a predominant organic acid present in urban aerosol and in the effluent of several industries. oxalic acid is widely used as a bleaching agent in pharmaceuticals and fiber sectors, as cleaning agent for pig iron, as precipitating agent for rare earth metals in film processing of aluminium alloys, as plasticizers for polymers, in leather tanning, as an auto radiator cleanser, as a disinfectant to control bacteria and in film processing of aluminium alloys, as plasticizers for polymers, in leather tanning, as an auto radiator cleanser, as a disinfectant to control bacteria and germs, and also as a grinding agent in marble polishing industries etc. [1].

In addition, oxalic acid is also used in waste water treatment, as a reducing agent for photography and ink removal, removal of rust stains from kitchen counter tops, plumbing fixtures and fabrics. It is a good substitute of acetic acid as colouring moderant for dye stuffs. In organic synthetic uses, oxalic acid is used in producing resins, urea-formaldehyde moulding powder, butadiene catalyst, in producing bacteriophage, preparation of raw material for porcelain capacitor and electronic equipment detergents and in photocatalytic effluent treatment [2]. It is also used in oil and gas industries [3] and sugar mills [4].

Oxalic acid as a dust or in solution irritates the eyes [5], mucous membranes and skin [6]. There is little reported information on industrial scale exposures [7, 8], although chronic inflammation of the upper respiratory tract [9] has been described due to exposure to hot vapours arising from oxalic acid [10]. Solutions are irritating to skin after prolonged exposure and may cause localized pain with cyanosis [11] of the fingers and even gangrenous changes. Splashes in the eye produce epithelial damage. Fatalities have been reported [12, 13] following ingestion of as little as 5 gm of acid; the onset symptoms are rapid including those of shock, collapse

and convulsions. There may be marked renal damage, with the deposition of calcium oxalate in the lumen of the renal tubules. The potassium and calcium salts of oxalic acid are found naturally in few vegetables i.e. in cabbage, spinach and rhubarb leaves and also in the bark of some species of eucalyptus tree. Oxalic acid is most abundant in the Ali mountain region [14] followed by oxalic and malonic acid which are the photochemical products from natural emission. Concentrations of oxalic acid in summers are 2 to 3 times higher. The soil from the agriculture waste burning contains large quantities of oxalic acid which is a major challenge for the environmentalists today. So the removal of oxalic acid from the waste water is therefore quite essential and important.

Fly-ash, a finely divided powdered byproduct from coal fired plant or biomass combustion facilities required ultimate disposal. The major constituents of fly-ash are silica, alumina, iron oxide, lime, magnesia and alkali in varying amount with some unburnt activated carbon. Besides these, some minor elements such as Hg, As, Ge, Ga and traces of heavy metals (Cr, Co, Cu, Pb, Mn, Ni, Zn) [15] and rare earths may also be present in fly ash. The glassy (amorphous) siliceous spherical particulates are the active portion of fly ash. Typically, fly ash is 30 – 50% glass and higher glass content in the form of quartz is also present in it. Other metal oxides such as Mn_2O_3, TiO_2 etc. [16] and minerals like mullite, hematite, ferrite and rutile in fly ash [17] are desirable from the point of view of reactivity.

Fly-ash has been employed as a low cost adsorbent for flue gas and water cleaning [18 -23] and many efforts have been made focused on heavy metals [24, 25] and dye adsorption [26, 27] on fly-ash particles. However no investigations have been reported on organic acids. In this paper we report use of fly-ash as an adsorbent by activating it, for the complete removal of oxalic acid from aqueous waste. Batch adsorption studies were carried out systematically and attempts have also been made to understand the adsorption equilibrium and kinetics.

2. Experimental

2.1 Materials and Methods

Class F fly ash, collected from KSTPS (Kota super thermal power plant), Rajasthan, was dried and sieved to obtain uniform particle size sample. Stock solution of oxalic acid of BDH make was prepared by doubly distilled water. Phenolphthalein was used as an indicator in this study.

2.2 Catalyst synthesis

The catalyst has been synthesized by adding 60 mL of 0.05 N NaOH to 40 gm of pure fly-ash sample. Chemical activation was carried out by continuous stirring of a mixture (NaOH and F.A) for 3 hr at 90 °C then washed to a neutral pH and dried in an oven.

2.3 Characterization

Both the initial i.e. pure fly ash (F.A) and the residue obtained after alkaline treatment i.e. activated fly-ash (AFA) were characterized mineralogically and micro structurally. Philips Expert XRD used for determining crystallite size. Samples were scanned at 2 θ range of 0 - 80° at a scanning rate of 0.04 s^{-1} [28]. FT-IR spectra of both the samples were recorded in the range 400 - 4000 cm^{-1} with a resolution of 4 cm^{-1}. Specific surface area, pore volume and pore size in the sample were determined from N_2 adsorption-desorption isotherms using NOVA 1000 E surface area at 77 K. Thermogravimetric analysis (TGA) was investigated in the temperature range 50 °C to 1000 °C using model Mettler Toledo. To determine the morphology, external surface structures and external elemental distribution of individual FA particle, scanning electron microscope (Philips XL 30 ESEM TMP) has been used.

2.4 Adsorption Kinetics

In the batch method, 50 mL of adsorbate solution was taken into an Erlenmeyer flask and allowed to attain the desired temperature by circulating thermostated water around the reaction vessel. To initiate the reaction, a fixed amount of adsorbent (2 gm dm^{-3}) was added and stirred continuously at about 1400±1 rpm. The kinetics was followed by withdrawing 0.05 dm^3 aliquot sample at different intervals.

Temperature was varied for estimating activation energy. Experimental runs were observed with initial rapid adsorption trends for a period of 30s to 2.5 min.

3. Results and Discussion

3.1 Characterization of adsorbent

3.1.1 XRD Analysis: The presence of quartz, mullite and calcite is witnessed in both FA and AFA (Fig 1 a, b).

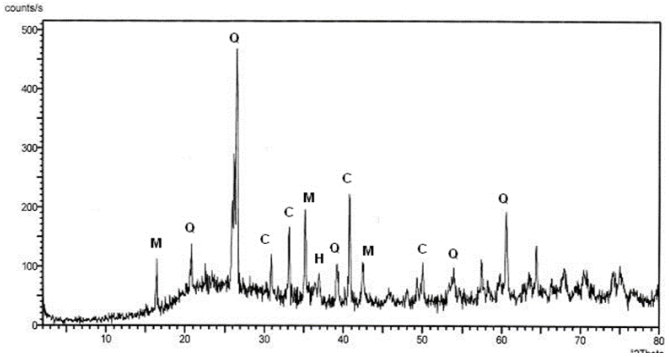

Fig 1(a): XRD of Pure Fly ash Q – Quartz, C- Calcite, M – Mullite, H- Haematite

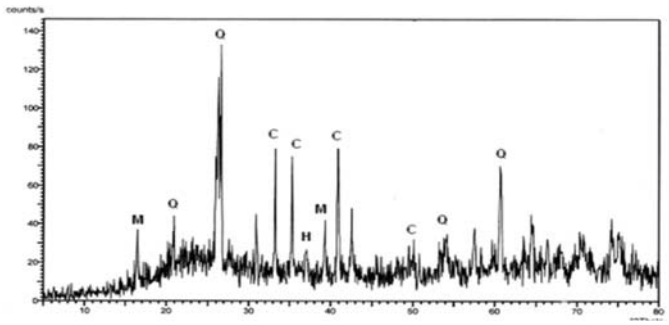

Fig 1(b): XRD of alkali activated Fly ash Q – Quartz, C- Calcite, M – Mullite, H- Haematite

Crystallite size decreased from 33 nm to 11 nm on NaOH treatment. It is evident from XRD study that chemical activation has removed most of the crystalline component present in the pure fly-ash thus lowering the crystallinity of the sample and increasing amorphous nature showed the presence of nanocrystalline phase in the sample. Previous studies have shown that fly ash after alkali treatment gives sharp diffraction peaks that are different from those present in untreated one. The diffractograms show the original crystalline phases of fly ash, quartz and mullite are mostly absent in zeolite material after reaction [29].

3.1.2 SEM Analysis: Fig 2(a) and (b) show the scanning electron microscope picture of pure and activated FA respectively. In addition to the general physical characteristics the elemental composition of random population of fly ash, the SEM data clearly indicate intermixing of silica and alumina phases and predominance of Ca and other non-silicate minerals. These results supported the data obtained from XRD. Fig 2(a) reveals that in the FA, the size of particles range from 840 nm to 10 µm and the majority of particles ranged in 1 µm to 100 µm, consisted of solid sphere, hollow cenosphere, irregularly shaped unburnt carbon particles and mineral aggregates and agglomerated particles which after alkali treatment (Fig 2b) resulted into scattered agglomerated particles conferring the increase in amorphous property. These results supported data obtained from previous studies and were consistent with XRD data [30].

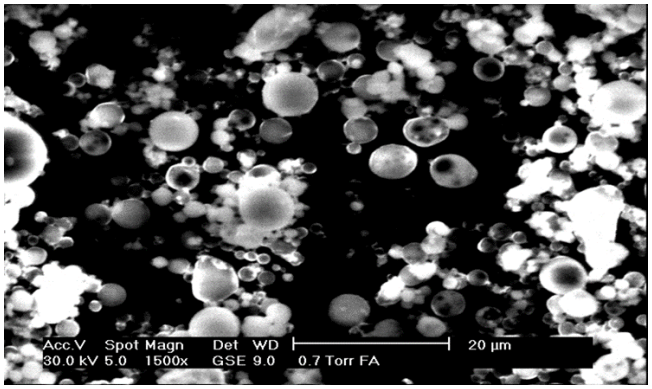

Fig 2(a): SEM Photograph of Pure Fly Ash

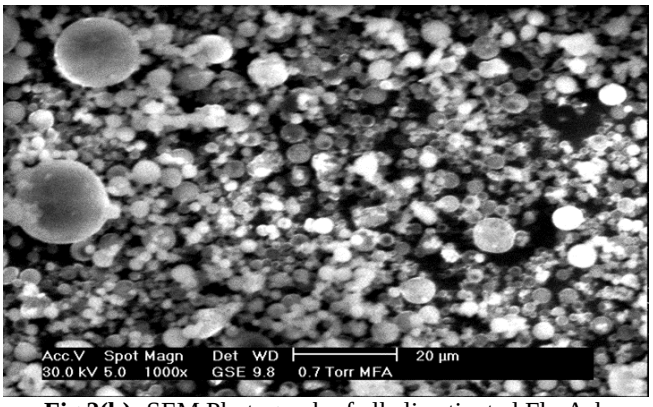

Fig 2(b): SEM Photograph of alkali activated Fly Ash

3.1.3 FT-IR Analysis

In alkali activation process higher concentration of –OH groups favor the breaking of Si-O-Si, Al-O-Al and Si-O-Al bonds and formation of Si-OH and Al-OH groups occur which is confirmed by a broad band between 3400 - 3000 cm^{-1} attributes the presence of surfacial hydroxyl group of –OH and adsorbed molecules on the surface. The broadening of a band is due to the strong hydrogen bonding. Signals at 996 cm^{-1}, 1081 cm^{-1}, 1185 cm^{-1} is attributed respectively to the vitreous phase of unreacted fly-ash, quartz and mullite while a new component appearing at around 1025 - 1006 cm^{-1} is attributed to the sodium aluminosilicate [31] which is also confirmed by some previous studied [32].

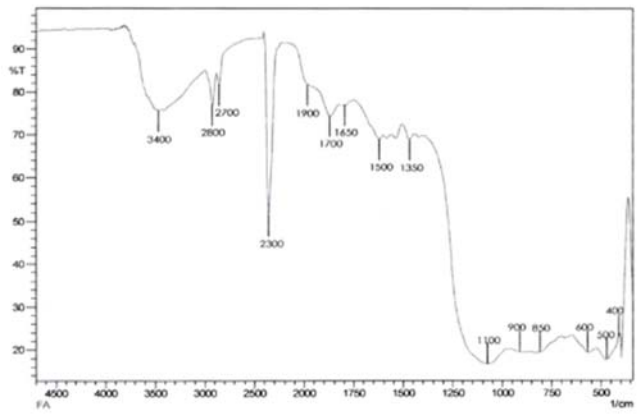

Fig 3(a): – FT-IR spectra of pure Fly Ash.

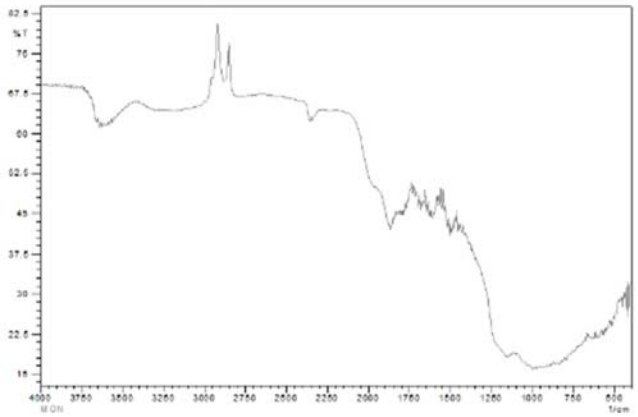

Fig 3(b): – FT-IR spectra of alkali activated Fly Ash.

3.2 Adsorption Isotherms

To optimize the design of an adsorption system for the adsorption of adsorbate, the most appropriate correlation for the equilibrium curve is Langmuir and Freundlich. The Langmuir isotherm is valid for monolayer adsorption onto a surface containing a finite number of identical sites.

$$Qe = \frac{Q_0 b C_e}{1+bC_0} \qquad \text{Eq. (A.1)}$$

Or

$$m/x = \frac{1}{Q_0} + \frac{1}{Q_0 b C_e} \qquad \text{Eq. (A.2)}$$

Where C_e is the equilibrium concentration in mg/L and Q_0 is the solid phase concentration corresponding to complete coverage of adsorption sites, b is the Langmuir constant, which indicates the nature of adsorption and indicates the shape of the isotherm accordingly. The essential characteristics of a Langmuir isotherm can be expressed in terms of a dimensionless separation factor (r) [33, 34], which describes the type of isotherm and is defined by equation (3)

$$r = \frac{1}{1+bC_0} \qquad \text{Eq. (A.3)}$$

Linearised Freundlich adsorption isotherm equation is given by equation (3)

$$\lg q_e = \lg K_f + 1/n \ \lg C_e \qquad \text{Eq.(A.4)}$$

Where q_e is the amount of acid adsorbed per unit weight of adsorbent (mg/g), K_f and 1/n are the Freundlich constants related to adsorption capacity and intensity respectively.

Table 1: Values of Langmuir and Freundlich constants for oxalic acid adsorption over AFA at different [acid] at 30 °C

10^{-3} [acid] mol dm^{-3}	Langmuir constants				Freundlich constant	
	b	*R*	Qo	R^2	K_f	1/n
5	1.045	0.18	39.37	1.0	117.5	0.3984
10	0.528	0.18	76.92	1.0	151.5	0.3992
50	0.100	0.19	169.4	1.0	1893.6	0.4921

The Langmuir plots are linear, shown in fig (4a). The plots of Freundlich isotherm yield a straight line of slope 1/n and intercept log K_f. It is clear from table 1 that the r values for the present experimental plot favors the adsorption of adipic acid on alkali activated fly ash.

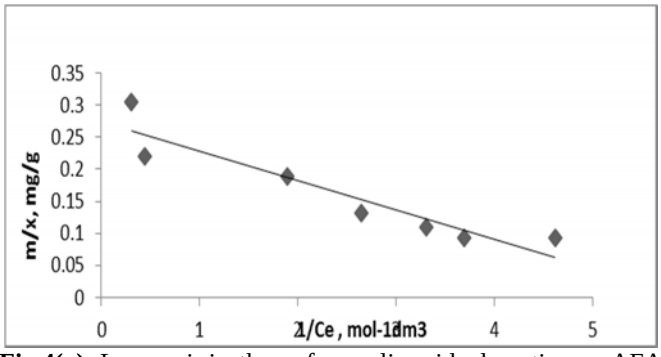

Fig 4(a): Langmuir isotherm for oxalic acid adsorption on AFA

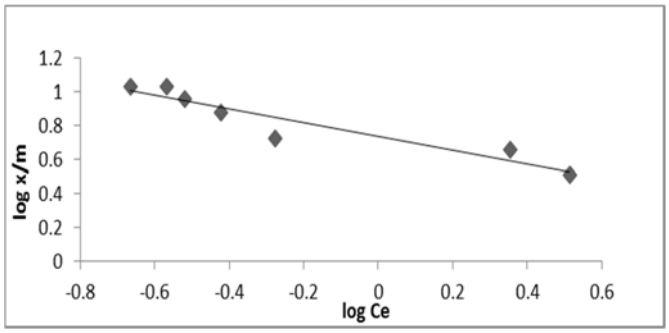

Fig 4(b): Freundlich isotherm for oxalic acid adsorption on AFA

3.3 Kinetics of adsorption

Kinetics of oxalic acid removal over AFA is studied by varying concentration of oxalic acid, AFA and temperature.

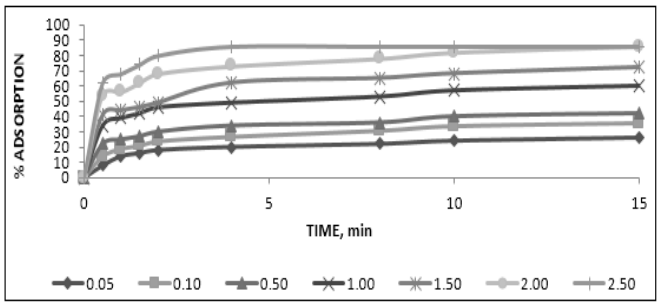

Fig 5: Change in % adsorption of oxalic acid with time at different *[AFA] at* 30 °C

Time v/s percentage adsorption graph shows (fig 5) initial rapid adsorption. Initial slope is used for determining initial rate (R_{obs}). From the log-log plot of R_{obs} v/s oxalic acid and R_{obs} v/s AFA, an order of 1.0 and 0.6±0.03 is achieved respectively. The functional dependence of rate on [acid] and [AFA], the final rate law is

$$R_{obs} = K[(CH_2)_4(COOH)_2]\,[AFA]^{0.6} \qquad \text{Eq. (B.1)}$$

The value of K is calculated 0.3475±0.13 g $dm^{-1.9}$ s^{-1} from the plot of R_{obs} with $[AFA]^{0.6}$.

Temperature was varied from 25 °C to 35 °C. The values of k determined at different temperature were used in Arrhenius equation. From the plot of log k against 1/*T*, the value of activation energy was calculated to be 43.54±2.15 kJ mol^{-1}.

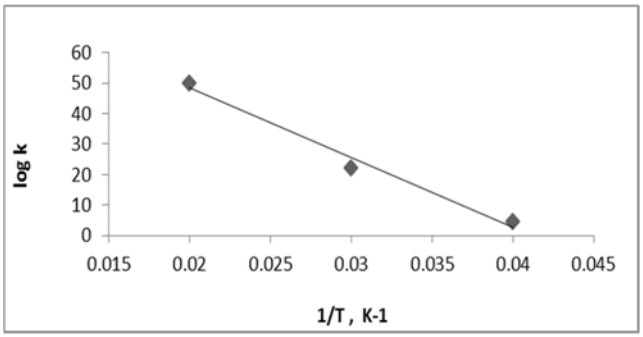

Fig 6: Arrhenius equation plot for oxalic acid adsorption

The above adsorption kinetics was modeled on five different models. All models were tested with least square regression analysis; values of statistical parameters for different examples are given in table 2.

On the basis of high values of R^2 and low SEE the most favorable model is first order kinetic model.

Table 2: Coefficient of determination (R^2), standard error of estimate (SEE), and slope for graphical equation of different kinetic models applied on oxalic acid adsorption on [AFA] at 30 °C.

[ACID]= 5×10^{-3} mol dm^{-3} , [AFA]= 2 g dm^{-3}			
Kinetic models	R^2	SEE	Slope
Zero order	0.5540	0.23569	-0.07
First order	0.9953	0.01034	-0.2182
Elovich equation	0.6073	0.12509	-0.0886
Parabolic diffusion	0.4922	0.41016	-0.4199
Two rate constant	0.5419	0.13100	-0.021

4. Conclusion

The adsorption catalyst AFA synthesized during this work is found to have sufficient activity to remove oxalic acid. Kinetic rate law has given first order with respect to initial concentration and a fractional order of 0.6±0.03 for [AFA] at 30 °C. A high value of activation energy indicates, chemisorption is to be important in case of using AFA than physisorption. The study generates fly-ash catalyst for waste water treatment in lubricants, plasticizer, pharmaceutical industries etc. where oxalic acid remains as waste in the effluent.

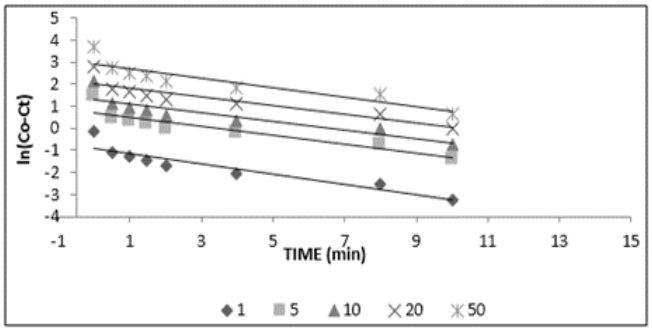

Fig 7: First order equation plots for oxalic acid adsorption at different [Acid]. [AFA]= 2.0 g dm^{-3} Temp. = 30 °C.

5. Acknowledgement

The authors are thankful to Dr. D.D. Phase and Er. V.K. Ahiray for SEM analysis, conducted at UGC DAU-CSR Lab Indore. The financial support was provided by Fly Ash Unit, Department of Science and Technology, New Delhi, India, vide project sanction no. FAU/DST/600(23)/2009-10.

6. References

1. Occupational Health Guideline for Oxalic acid, U.S. Department of Health and Human services, U.S. Department of Labour, 1978.

2. Tarasova II, Dudeney AWL, Pilurzu S. Glass sand processing by Oxalic acid Leaching and Photocatalytic Effluent Treatment. Minerals Engineering 2001; 14(6):639-646.
3. Irawan S, Samsuri A. Extraction of Mononitrile Mineral Iron oxide with Organic acid. Universitas Islam Riau (UIR), Universiti Technology Malaysia (UTM), Proceedings of Indonesian Petroleum Engg Association, 2003.
4. Sethi A. Poor Industrial Practices and a Myopic Environmental Policy Lead to the Pollution of North India's Water Resource. Frontline, Indian national magazine 2007; 14-27.
5. Grant WM. Toxicology of the Eye. Edn 2, CC Thomas, Springfield, Illinois, 1974.
6. Schwartz L, Tulipan L, Birmingham D. Occupational Disease of the Skin. Edn 3. Rev, Lea and Febiger, Philadelphia, 1957.
7. American Conference of Governmental Industrial Hygienists, "Oxalic acid". Documentation of the Threshold Limit Value for Substances in Workroom Air. Edn 3, Cincinati, 1974.
8. Fairhall LT. Industrial Toxicology. Edn 2, Williams and Wilkins, Baltimore 1957.
9. Howard C. Chronic Poisoning by Oxalic acid. Journal of an Industrial Hygiene 1932; 14(8):283-290.
10. Gleason MN, Gosselin RE, Hodge HC, Smith RP. Clinical Toxicology of Commercial Products. Edn 3, Williams and Wilkins, Baltimore, 1969.
11. Deichmann WB, Gerarde HW. Toxicolgy of Drugs and Chemicals. Academic Press, Newyork, 1969.
12. International labour office. Encyclopedia of National Health and Safety. McGraw Hill, Newyork, 1971.
13. Patty FA. Toxicology, Industrial Hygiene and Toxcology. Edn 2, Rev., Vol. 2, Interscience New York, 1963.
14. Vogel AI. A Text Book of Analysis. Longman Green, London, 357-370.
15. Mallik D, Khanra S , Chaudhury SK. Studies on the potential of coal fly ash as a heterogeneous catalyst in oxidation of aqueous sodium sulfide solutions with hydrogen peroxide. J Chem Technol Biotechnol 1997; 70:231-240.
16. Kumar K, Kumar S, Mehrotra SP. Towards sustainable solutions for fly ash through mechanical activation. Resourse Conserv. Recycl 2007; 52:157-179.
17. Karapanagioti HK, Atalay AS. Laboratory Evaluation of Ash Materials as Acid-Disturbed Land Amendments. Gl Nest: The Int 2001; 3:11-21.
18. Kastener JR, Melear ND, Das KC. Catalytic Oxidation of Gaseous Reduced Sulphur Compounds Using Coal Fly ash. J Hazardous Material 2002; 95:81-90.
19. Lu GQ, Do DD. Adsorption Properties of Fly ash Particles for NO_x Removal from flue Gases. Fuel Process Technol 1991; 27(1):95-107.
20. Carry TR, Richardson CF, Chang R, Meserole FB, Rostam M Abadi, Chen S. Assessing Sorbent Injection Mercury Control Effectiveness in Flue Gas Streams. Environ Prog 2000; 19:167-174.
21. Malerius O, Werther J. Modeling the Adsorption of Mercury in the Flue gas of Sewage sludge Incineration. Chem Eng J 2003; 96:197-205.
22. Peloso A, Rovatti M, Ferraiolo G. Fly ash as Adsorbent Material for Toluene Vapours. Resour Conserv 1983; 10:211– 220.
23. Panday KK, Prasad G, Singh VN. Copper(II) Removal from Aqueous Solutions by Fly ash. Water Res 1985; 19:869-873.
24. Sen AK, De AK. Adsorption of Mercury(II) by Coal Fly ash. Water Res 1987; 21:885-888.
25. Mohan D, Singh KP, Singh G, Kumar K. Removal of Dyes from Waste Water using Fly ash, a Low Adsorbent. Ind Eng Chem Res 2002; 41:3688-3695.

26. Janos P, Buchtova H, Ryznarova M. Sorption of Dyes from Aqueous Solutions onto Fly ash. Water Res 2003; 37:4938-4944.
27. Cullity BD, Stock SR. Elements of X-Ray Diffraction. Prentice Hall. Edn 3, 2001.
28. Postek MT, Howard KS, Johnson AH, Michael KL. Scanning Electron Microscopy: A students Handbook Burlington, Ladd Research Industries, 1980.
29. Ojha K, Narayan CP, Samanta A. Zeolite from fly ash: Synthesis and characterization. Bull Mate Sci 2004; 27:555-564.
30. Barbara G, Kutchko, Ann GK. Fly ash characterization by SEM-EDS. Fuel 2006; 85:2537-2544.
31. Fernandez AJ, Palomo A. Mid Infrared Spectroscopic Studies of Alkali Activated Fly ash Structure. Microporous and Mesoporous Material 2005; 86(1-30):207-208.
32. Fernandez AJ, Monzo M, Vincent M, Barba A, Palomo A. Alkaline Activation of Metakaolin-Fly ash mixtures: obtained from Zeoceramics and Zeocements. Microporous and Mesoporous Materials 2008; 108:41-49.
33. Weber TW, Chakravorti RK. Pore and Solid Diffusion Models for Fixed Bed Adsorber. J Am Ins Chem Eng 1974; 2:228-238.
34. Kanan N, Sundaram M. Kinetics of Adsorption of Dyes on CAC. Ind J Env Protec 2002; 22(1):9-11.